Z. Phys. A 350, 303–309 (1995)

ZEITSCHRIFT
FÜR PHYSIK A

The ^{115}In(γ, γ') reaction as a test of the quasi-particle phonon model with complex configurations in odd-mass nuclei

P. von Neumann-Cosel, V.Yu. Ponomarev*, A. Richter, C. Spieler

Institut für Kernphysik, Technische Hochschule Darmstadt, Schlossgartenstrasse 9, D-64289 Darmstadt, Germany

Received: 9 August 1994

Abstract. The ^{115}In(γ, γ') reaction was measured at the S-DALINAC using bremsstrahlung with endpoint energies $E_0 = 3.1$, 4.6 and 5.2 MeV. In the excitation energy range of 1–5 MeV in total 32 transitions were observed, 18 of which were hithertoo unknown. The results are compared to two quasiparticle-phonon model calculations, one with a model space of 'quasiparticle⊗phonon' and one extended by 'quasiparticle⊗two-phonon' configurations. A substantial improvement is achieved in the description of low-lying ^{115}In states by the consideration of the more complex configurations. The calculations quantitatively account for the summed ^{115}In(γ, γ') integrated cross sections and show a comparable amount of fragmentation of the individual transition strengths. The model interpretation of the microscopic structure of the experimentally observed transitions is discussed.

PACS: 21.10.Tg; 21.60.−n; 25.20.Lj; 27.60.+j

1. Introduction

Recently, numerous experimental investigations of inelastic photon scattering in odd-even nuclei have been reported. The interest has focused e.g. on the identification of the orbital magnetic dipole "scissors" mode in heavy deformed nuclei [1, 2] and the first proof of a pure 'two-phonon ⊗ particle' structure in ^{143}Nd [3]. The present work on ^{115}In was motivated by systematic studies of the photoexcitation of spin isomers [4, 5] which typically show a few intermediate states with large cross sections. It was demonstrated in [6] for the example of ^{115}In that the combination of nuclear resonance fluorescence data with photoactivation results yields important insight into the structure of the intermediate levels.

A satisfactory description of the gross features was achieved with a semiempirical unified model (UM) approach [7]. However, a detailed description of the relevant amplitudes describing resonant photon scattering to the ground state and/or to an isomer in odd-mass nuclei crucially depends on a delicate interplay of collective and single particle degrees of freedom. Electromagnetic transitions provide particular stringent model tests because of their sensitivity to small amplitudes in the initial and final state wave functions. Because of model inherent approximations the predictive power of the UM for such data is certainly limited.

Therefore, besides a full presentation of the experimental results of the ^{115}In(γ, γ') reaction the present work concentrates on a description of the resonant photon scattering results within the microscopic quasiparticle-phonon model (QPM). The QPM has been able to explain successfully the nature of intermediate structures in the photoexcitation of isomers taking into account a 'quasiparticle ⊗ phonon' model space [5, 8–10]. In a study of ^{89}Y good agreement for the total (γ, γ') strength, but too little fragmentation was observed which was traced back to the omission of more complex configurations [10]. Here, an extension of the model is described to include 'quasiparticle ⊗ two-phonon' states in the calculations of electromagnetic transitions and its importance for a detailed description is tested with the ^{115}In(γ, γ') data set.

2. Experiments

The measurements were performed at the injector of the superconducting electron linear accelerator S-DALINAC at Darmstadt [11]. Electron with energies $E_0 = 3.1$, 4.6 and 5.2 MeV bombarded a rotating 3 mm thick tantalum converter to produce bremsstrahlung. Typical electron currents were 20 μA. The photons scattered from the target were detected with two well-shielded hpGe, respectively Ge(Li), detectors placed under 90° and 127°.

The targets consisted of ^{nat}In disks of 8.3–10.2 g with a diameter of 1 cm. Disks of total 1 g ^{nat}Al (for $E_0 = 3.1$

* *Permanent address:* Laboratory for Theoretical Physics, Joint Institute for Nuclear Research, Dubna, Head Post Office, P.O. Box 79, Moscow, Russia

and 4.6 MeV) and 0.205 g ^{nat}B (for $E_0 = 5.2$ MeV) were sandwiched around the targets. The well known (γ, γ') transitions of ^{27}Al and ^{11}B served as a reference for the determination of the bremsstrahlung spectral shape and total photon flux [12, 13]. Further experimental details can be found in [14].

3. Experimental results

The spectra recorded at the three bremsstrahlung endpoint energies are displayed in Fig. 1. Transitions which are attributed to the ^{115}In (γ, γ') reaction are marked by arrows. The line contents were converted to experimental integrated cross sections as described e.g. in [15]. The bremsstrahlung spectra were calculated with the Monte Carlo program GEANT3 [16] and normalized to the ^{27}Al and ^{11}B reference transitions. The validity of the Monte Carlo results for the description of low energy, thick target bremsstrahlung has recently been confirmed with independent experimental methods [17].

All identified ^{115}In transitions were assumed to be g.s. transitions. The observation of transitions to excited states

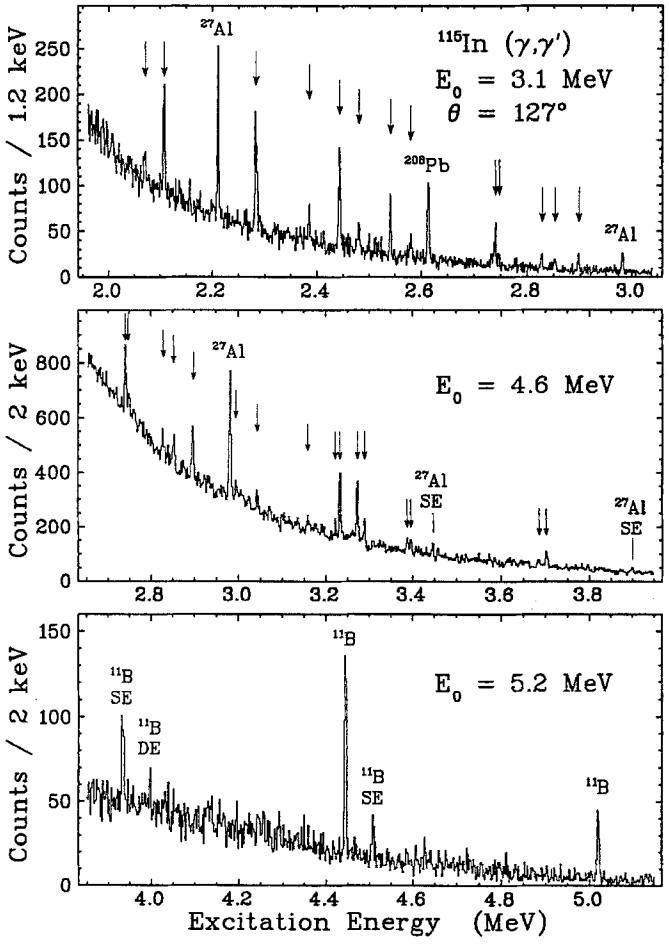

Fig. 1. Spectra of the ^{115}In (γ, γ') reaction at three different bremsstrahlung endpoint energies. Transition assigned to ^{115}In are marked by *arrows*. The symbols SE and DE denote single- and double-escape lines, respectively

can be largely excluded in the present case. Because of the restriction to low multipolarities ($\lambda = 1, 2$) in nuclear resonance fluorescence (NRF) the lowest states which could be efficiently populated would be the $E_x = 0.934$ MeV, $J^\pi = \frac{7}{2}^+$ level [18]. Such transitions with correspondingly reduced γ-energies would be covered by the Compton background which rises roughly exponentially towards lower energies.

The integrated cross sections I_s are related to the decay width Γ by

$$I_s = \pi^2 \left(\frac{\hbar c}{E_\gamma}\right)^2 g \frac{\Gamma_0^2}{\Gamma} W(\Theta), \tag{1}$$

where Γ_0 denotes the partial g.s. decay width, $g = (2J_i + 1)/(2J_0 + 1)$ is the statistical factor with J_0, J_i the spins of the g.s. and the excited state, respectively, and $W(\Theta)$ accounts for the nonisotropic decay which depends on the multipolarity and the $E2/M1$ mixing ratio.

Table 1 summarizes the observed transitons together with the results of previous ^{115}In NRF studies [19–21] and other information on the level properties available in the literature [18]. Unlike the case of even-even nuclei where the ratio of results obtained at 90° and 127° permits a distinction between dipole and quadrupole transitions, the angular distributions $W(\Theta)$ are much more isotropic in odd-even nuclei. It is found for ^{115}In that under 127° for all possible spin combinations $\frac{9}{2} \rightarrow (\frac{5}{2} - \frac{13}{2}) \rightarrow \frac{9}{2}$ and $E2/M1$ mixing ratios, $W(\Theta)$ varies less than 10% from unity. Therefore, the results in Table 1 are taken from the 127° detector and the angular dependence is neglected. Instead an additional systematic error of 10% should be added to the errors given.

In general, the present results compare well with previous work for $E_x < 2$ MeV where partial widths can be calculated from the known level properties. Exceptions are the transitions to the $E_x = 1.078$, 1.449 and 1.497 MeV states. The two former show larger partial widths than extracted from other experimental data [18], most likely because of additonal feeding through higher-lying states. For the transition to the $E_x = 1.497$ MeV level the integrated cross section is a factor of about 2.5 smaller. However, one should be aware that even for the lowest endpoint energy $E_0 = 3.1$ MeV the peak-to-background ratio at this energy is already poor and that the strength was close to the detection limit.

The agreement with previous ^{115}In (γ, γ') work is mixed. Good correspondence is observed for the 1.608 MeV level measured by Cauchois et al. [21], while the deviations for the 1.497 MeV transition are discussed above. The results of Alston [19] agree within errors for the 2.480 and the 2.740 MeV transitions, but are significantly smaller for the 2.283 MeV and the 2.443 MeV transitions. Above $E_x = 3.8$ meV no transitions belonging to ^{115}In could be identified. From the statistics an experimental upper limit $g \frac{\Gamma_0^2}{\Gamma} \leqq 7$ meV at $E_x = 4$ MeV rising to ≈ 45 meV at $E_x = 5$ MeV is estimated.

Table 1. Transition observed in the $^{115}In(\gamma,\gamma')$ reaction and comparison to previous work

This work			Other $^{115}In(\gamma,\gamma')$ work			Literature		
			[21]	[20]	[19]	[18]		
E_x (MeV)	I_s (eVb)	$g\frac{\Gamma_0^2}{\Gamma}$ (meV)	$g\frac{\Gamma_0^2}{\Gamma}$ (meV)	$g\frac{\Gamma_0^2}{\Gamma}$ (meV)	$g\frac{\Gamma_0^2}{\Gamma}$ (meV)	E_x (MeV)	J^π	$g\frac{\Gamma_0^2}{\Gamma}$ (meV)
1.0781(3)	1.4 (5)	0.42(15)	0.159(24)		0.31 (9)	1.0782 (3)	$\frac{5}{2}^+$	0.19 (1)
1.1326(2)	28.1(21)	9.4 (7)	8.59 (48)	6.3 (6)	6.3 (11)	1.1326 (0)	$\frac{11}{2}^+$	8.4 (4)
1.2908(2)	2.9 (6)	1.2 (3)	1.31 (11)	0.95(44)	1.35(35)	1.2906 (0)	$\frac{13}{2}^+$	1.45(14)
1.4489(3)	3.1 (5)	1.7 (4)	0.90 (11)	0.91(38)	0.7 (2)	1.4488 (0)	$\frac{9}{2}^+$	0.94(11)
1.4630(2)	8.9(11)	4.0 (6)	5.22 (66)	7.7 (20)		1.4633 (7)	$\frac{7}{2}^+$	5.1 (8)
1.4867(2)	1.4 (4)	0.80(21)	0.63 (9)	0.88(22)		1.4861 (1)	$\frac{9}{2}^+$	0.66 (9)
1.4970(3)	0.8 (3)	0.49(18)	1.33 (16)		1.6 (6)	1.4972 (8)	$\frac{7}{2}^+$	1.33(16)
1.6080(3)	1.5 (4)	1.0 (3)				1.6081 (7)	$\frac{7}{2}^+$	1.54(24)
2.0710(4)	1.3 (3)	1.4 (4)				2.0710(10)	$(\frac{5}{2}^+)$	
2.1078(2)	4.4 (5)	5.1 (6)				2.1077(15)	$(\frac{5}{2}^+)$	
2.2830(2)	9.1 (9)	12.4 (13)			7.0 (23)	2.277 (5)		
2.3846(3)	2.8 (5)	4.1 (7)						
2.4431(2)	9.5(10)	14.8 (16)			5.6 (19)	2.438 (5)		
2.4797(3)	3.3 (5)	5.2 (8)			4.7 (19)	2.476 (5)		
2.5407(2)	6.5 (8)	10.9 (14)						
2.5800(3)	2.9 (5)	5.0 (9)						
2.7399(2)	8.1(12)	15.8 (24)			12.6 (42)	2.742 (5)		
2.7467(4)	2.5 (6)	4.9 (12)						
2.8275(3)	2.5 (6)	5.1 (13)						
2.8522(4)	3.4 (6)	7.1 (14)						
2.8967(4)	6.6 (9)	14.5 (19)						
2.9944(6)	2.8 (6)	6.5 (14)						
3.0429(5)	2.8 (7)	6.8 (18)						
3.1582(7)	2.0 (5)	5.2 (14)						
3.2207(6)	2.3 (6)	6.2 (15)						
3.2315(3)	11.9(11)	32.4 (29)						
3.2719(3)	12.4(11)	34.6 (31)						
3.2885(4)	4.0 (6)	11.2 (18)						
3.3865(5)	2.3 (6)	7.0 (8)						
3.3950(5)	2.7 (6)	8.2 (18)						
3.6846(9)	3.5(10)	12.5 (35)						
3.7010(5)	7.7(13)	27.3 (47)						

4. Quasiparticle-phonon model calculations

4.1. Formalism and details of the calculations

The general description of the QPM application in treating odd nuclei can be found e.g. in [22]. Here we only briefly outline the major ideas of this model important for the specific calculations and present recent developments of the model.

The ground and excited states of odd-mass nuclei are considered by the QPM in terms of 'free' quasiparticles described by the quasiparticle creation operator α^+_{jm} and quasiparticles coupled to phonon excitations of the neighbouring even-even core, with the respective phonon creation operator $Q^+_{\lambda\mu i}$. Here, jm stands for the quantum numbers of the single-particle state in the average field and $\lambda\mu$ are boson quantum numbers of core excitations; i numbers the sequence of one-phonon states for definite λ^π. Since these simple modes are mixed in a real nucleus, the wave function is written as a composition

$$\begin{aligned}\Psi_\nu(JM) &= C^\nu_J\left\{\alpha^+_{JM}+\sum_{\lambda ij} D^{\lambda i}_j(J\nu)[\alpha^+_{jm}Q^+_{\lambda\mu i}]_{JM}\right.\\ &+\sum_{\lambda_1 i_1\lambda_2 i_2 jJ'} F^{\lambda_1 i_1\lambda_2 i_2}_{jJ'}(J\nu)\\ &\left.\times[\alpha^+_{jm}[Q^+_{\lambda_1\mu_1 i_1}Q^+_{\lambda_2\mu_2 i_2}]_{J'M'}]_{JM}+\ldots\right\}\Psi_0,\end{aligned}\tag{2}$$

where Ψ_0 is the wave function of the g.s. of the neighbouring even-even core and ν is the order number of excited states with spin J. The amplitudes C^ν_J, $D^{\lambda i}_j(J\nu)$ and $F^{\lambda_1 i_1\lambda_2 i_2}_{jJ'}(J\nu)$ for each state are obtained from a diagonalization with an effective Hamiltonian. It includes

an average field for protons and neutrons $V_{p,n}$, a monopole pairing interaction, and isoscalar and isovector residual interactions of a separable type with a form factor proportional to $\mathrm{d}V_{p,n}/\mathrm{d}r$.

Diagonalization of the Hamiltonian yields a set of equations for excitation energies η_{Jv} and coefficients $D_j^{\lambda i}(Jv)$ which can be written in a matrix form as

$$\varepsilon_J - \eta_{Jv} - \frac{1}{\sqrt{2}} \Gamma \times D = 0, \tag{3}$$

$$D \times M(\eta_{Jv}) = \frac{1}{\sqrt{2}} \Gamma. \tag{4}$$

The dimension of the array $D = \{D_{j_1}^{\lambda_1 i_1}(Jv), D_{j_2}^{\lambda_2 i_2}(Jv), \ldots\}$ is determined by the number of 'quasiparticle ⊗ phonon' configurations included in the wave function (2). The array $\Gamma = \{\Gamma(Jj\lambda i), \ldots\}$ includes matrix elements of the interaction between quasiparticle configuration α_J^+ and quasiparticle ⊗ phonon configurations $[\alpha_j^+ Q_{\lambda i}^+]_J$ which are calculated microscopically. The explicit form of $\Gamma(Jj\lambda i)$, as well as a complete description of the matrix $M(\eta_{Jv})$ can be found in [22]. Also relations between the coefficients $F_{jJ'}^{\lambda_1 i_1 \lambda_2 i_2}(Jv)$ and $D_j^{\lambda i}(Jv)$ and the determination of C_J^v from the normalization of the wave function (2) are presented there.

An important point in treating the core excitations as boson-like phonons is a possible violation of the Pauli principle because of the underlying fermion structure

$$Q_{\lambda\mu i}^+ = \tfrac{1}{2} \sum_{jj'}^{p,n} \{\psi_{jj'}^{\lambda i} [\alpha_{jm}^+ \alpha_{j'm'}^+]_{\lambda\mu} + (-1)^{\lambda-\mu} \varphi_{jj'}^{\lambda i} [\alpha_{jm} \alpha_{j'm'}]_{\lambda-\mu}\}. \tag{5}$$

The forwardgoing $\psi_{jj'}^{\lambda i}$ and backwardgoing $\varphi_{jj'}^{\lambda i}$ amplitudes are obtained by solving the random phase approximation (RPA) equations which also yield the energies of the phonon excitations. To avoid problems of this kind, a special technique has been developed [23] within the QPM by using exact commutation relations between quasiparticles and phonons. It results in a renormalization of the interaction between quasiparticles and phonons and in a shift of energetic locations of $[\alpha_j^+ Q_{\lambda i}^+]_J$ and more complex configurations.

Until now, (3, 4) were solved only in deformed nuclei for a very truncated quasiparticle and phonon basis [24]. Usually, either 'quasiparticle ⊗ two-phonon' configurations were omitted in the wave function [23, 25, 26] or a strength function method was used to include them directly [22]. Alternatively, one can make use of a phenomenological optical potential [27]. The strength function method rather simplifies the calculations but yields only a general distribution of strength of the investigated configuration over excitation energy and does not allow to extract the structure information on each excited level. We aim here to develop a theoretical working scheme on a microscopic basis which takes into account complex configurations of the wave function and preserves the knowledge of the structure of excited states in odd nuclei at low and intermediate energies (typically up to $E_x = 4 - 5$ MeV).

We include for the third term in (2) configurations $[\alpha_j^+ [Q_{\lambda_1 i_1}^+ Q_{\lambda_2 i_2}^+]_{J'}]_J$ built on collective low-lying phonons, viz. $\lambda_1 i_1$, $\lambda_2 i_2 = 2_1^+$, 3_1^- and 4_1^+ in all possible combinations. The influence of the Pauli principle violation for these terms has been included by calculating the energy shift and equals to at most a few hundreds keV for some configurations. A renormalization of the interaction between quasiparticles and phonons would not exceed a few per cent and is neglected. This is in an agreement with the role of the Pauli principle for 'quasiparticle ⊗ phonon' configurations [23]. Omitted non-collective terms interfere only weakly with other configurations. Also the contributions of other collective phonons which appear above about 3 MeV are not very important for the considered excitation energy region.

For 'quasiparticle ⊗ phonon' configurations the same basis truncation as in previous studies [5, 8, 10] is used, i.e. all configurations with energies less than 11 MeV constructed from both collective and non-collective phonons with $J^\pi = 1^+$, 2^+, 3^-, 4^+, 5^- and 6^+ are included. The Pauli principle corrections were calculated in a complete form. The number of $[\alpha_J^+ Q_{\lambda i}^+]_J$ and $[\alpha_j^+ [Q_{\lambda_1 i_1}^+ Q_{\lambda_2 i_2}^+]_{J'}]_J$ configurations in actual calculations varied from 47 and 43 for $J^\pi = \frac{1}{2}^-$ to 147 and 115 for $J^\pi = \frac{7}{2}^+$, respectively.

Equations (3, 4) are solved in the diagonal approximation as proposed in [28]. The matrix elements $M_{i,j}$ are set to zero for $i \neq j$. Non-diagonal terms play no important role because of their non-coherent nature which was proved by calculations in a truncated basis [24]. This approximation sufficiently simplifies numerical calculations because it yields a single non-linear equation (although with a complicated energy dependence) instead of a coupled system. Technically it was realised on the basis of the computer code PHOQUS [29].

4.2. *Description of low-lying levels*

The effect of an inclusion of two-phonon coupled states on the description of low-lying levels is demonstrated in Fig. 2. With the one-phonon coupled model space large discrepancies are observed for all levels above $E_x \approx 0.8$ MeV. This effect is nicely corrected by the inclusion of the more complex configurations, in particular for the positive parity rotational-like sequence of intruder states [25]. Also, the inversion of the lowest $J^\pi = \frac{3}{2}^-$, $\frac{3}{2}^+$, $\frac{1}{2}^+$ states is removed.

The role of complex configurations is most essential for states with a large contribution of $[\alpha_j^+ Q_{\lambda i}^+]_J$ configurations where $\lambda i = 2_1^+$, 3_1^- or 4_1^+. The interplay with complex configurations results in a shift of these states to lower energies. The same effect takes place in even-even nuclei when mixing of one- and two-phonon configurations is taken into account. It can be qualitatively explained in a simple two-level model where the interaction between these levels leads to repulsion. The parameters of the residual interaction were adjusted in the present calculation to reproduce the collectivity of the lowest 2_1^+ and 3_1^- states in neighbouring even-even nuclei, i.e. fixed to the experimental $B(E\lambda)$ values. Using

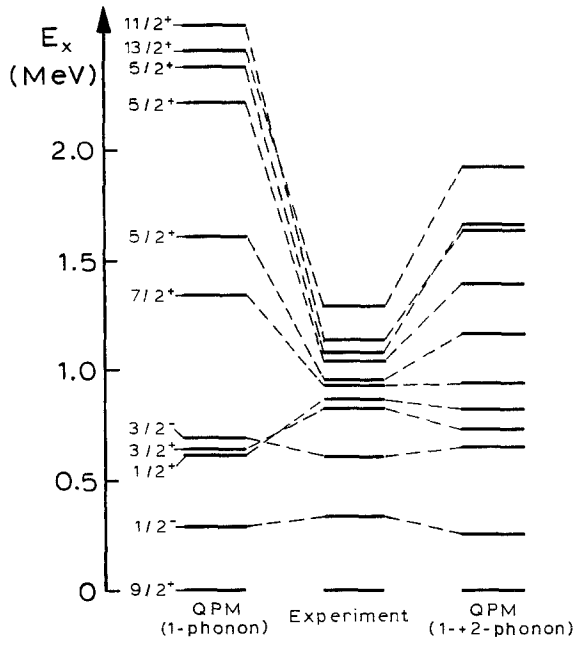

Fig. 2. Experimental low-energy spectrum of ^{115}In compared to QPM results without (1-phonon) and with (2-phonon) consideration of 'quasiparticle ⊗ two-phonon' configurations

these values the lowest RPA 2_1^+ and 3_1^- phonons have an energy which is a few hundred keV higher than the experimental ones. It is not surprising that in the odd-even ^{115}In nucleus the low-lying levels, which have a large contribution of the [g.s. ⊗ 2_1^+] configuration, show the same deficiency in the one-phonon coupled model space. Coupling to complex configurations restores the correct position of the lowest levels in both neighbouring even-even and odd-even nuclei.

The QPM also reasonably accounts for electromagnetic transition strengths. In Table 2 a comparison to experimental values is presented for transitions between g.s. and excited states up to about 1.5 MeV. For higher excitation energies the assignments are unclear. Good agreement is observed except for the transition to the lowest $J^\pi = \frac{7}{2}^+$ states. The differences of the two calculations are not very large but the inclusion of 'quasiparticle ⊗ two-phonon' configurations generally leads to a reduction of B-values which in most cases brings the calculations in closer agreement with the experimental data. The structure and mixing of the lowest $J^\pi = \frac{7}{2}^+$ states cannot be fully explained in the present approach. However, if one assumes the lowest theoretical $\frac{7}{2}^+$ level to correspond to the second experimental one, the agreement would be improved.

4.3. *Comparison to the* (γ, γ') *results*

In Fig. 3 the experimental integrated cross section observed in the ^{115}In(γ, γ') experiments are compared to QPM calculations in the energy range $E_x = 2-4$ MeV. The differences between the results with a one-phonon

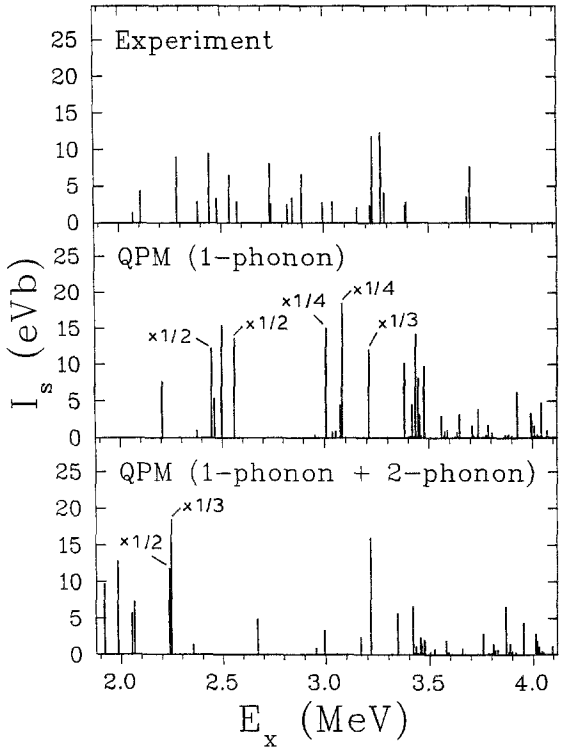

Fig. 3. Experimental integrated cross sections observed in the ^{115}In(γ, γ') experiment compared to QPM calculations taking into account 'quasiparticle ⊗ one-phonon' (1-phonon) and additonally two-phonon (1-phonon + 2-phonon) coupled states

Table 2. Comparison of experimental results and QPM calculations including 'quasiparticle ⊗ one-phonon' (1-phonon) and additionally 'quasiparticle ⊗ two-phonon' (1-+2-phonon) configurations for g.s. transitions to low-lying levels in ^{115}In

Literature [18]				QPM (1-phonon)		QPM (1-+2-phonon)	
E_x (MeV)	J^π	$B(M1)$ (W.u.)	$B(E2)$ (W.u.)	$B(M1)$ (W.u.)	$B(E2)$ (W.u.)	$B(M1)$ (W.u.)	$B(E2)$ (W.u.)
0.934	$(\frac{7}{2}^+)_1$	4.7×10^{-4}	2.0×10^{-4}	2.0×10^{-4}	6.8	1.3×10^{-4}	6.2
0.941	$(\frac{5}{2}^+)_1$		1.32		6.9		5.6
1.078	$(\frac{5}{2}^+)_2$		11.1		3.4		6.3
1.132	$(\frac{11}{2}^+)_1$	0.19	29	≈0	15.7	≈0	13.2
1.291	$(\frac{13}{2}^+)_1$		11.1		16.0		12.6
1.448	$(\frac{9}{2}^+)_3$	2×10^{-4}	4.5	0.11	11.2	0.25	8.8
1.463	$(\frac{7}{2}^+)_2$	0.05	1.7	3.4×10^{-4}	≈0	4×10^{-4}	≈0

and a one- plus two-phonon coupled model space are significant. While calculations with the restricted model space overpredict the summed integrated cross sections by a factor of about two, good quantitative agreement is obtained with inclusion of the more complex configurations. The main effect is a shift of some strong transitions around 2.5 and 3 MeV, which have no experimental counterpart, to lower energies. The degree of fragmentation of the cross sections with the full calculation is similar to the experimental results, although the main strength is shifted a few hundred keV to lower, respectively higher excitation energies.

It is of interest to discuss in more detail the sources of electromagnetic transition strength predicted by the QPM. In the full calculations about 50% of the summed integrated cross sections corresponds to $M1$ strength and the rest is about equally distributed between $E1$ and $E2$ strength. The major part of $M1$ excitations is of $g_{9/2} \rightarrow g_{9/2}$ type and only one transition ($E_x = 3.21$ MeV) of $g_{9/2} \rightarrow g_{7/2}$ spin-flip type. The $B(E2)$ strenght is due to coupling to the collective 2_1^+ states in the neighbouring ^{114}Cd and ^{116}Sn cores. The rather fragmented $E1$ strength is of $g_{9/2} \rightarrow f_{7/2}$ (and to a lesser extent $g_{9/2} \rightarrow h_{11/2}$) nature.

Thus, the QPM leads to a somewhat different interpretation compared to the UM [7] calculations described in [6]. There, the $B(M1)$ strength came solely from spin-flip transitions and no significant $B(E2)$ strength appeared (which, however, might be due to a systematic shortcoming of the UM, see [6]). At low excitation energies the QPM results show a dominance of $[2_1^+ (\mathrm{Cd}) \otimes g_{9/2}]$ configurations in contradiction to the UM where the Sn-coupled multiplet is more important. This difference results from the consideration of corrections due to the Pauli principle (see Sect. 4.1) neglected in the UM which shift the $[2_1^+ (\mathrm{Sn}) \otimes g_{9/2}]$ contributions to higher energies.

In the investigated energy range, $\sum B(M1) \approx 0.8 \mu_N^2$ according to the QPM results with the strength mainly concentrated in three transitions at $E_x = 1.99$, 2.25 and 3.21 MeV which have $B(M1) = 0.13$, 0.45 and $0.11 \mu_N^2$, respectively. Experimentally, the strength must be more fragmented. Assuming pure $M1$ excitation the strongest experimental transition would be at $E_x = 2.283$ MeV with $B(M1) = 0.10 \mu_N^2$. Very little other information exists on $B(M1)$ strength distribution in the $A = 110$–120 mass range. A high-resolution (e, e') study on ^{110}Pd for $E_x \leqq 4$ MeV has been reported [30], but gave only weak evidence for $M1$ strength. However, the experimental upper limit in [30] for a single $B(M1)$ transition was given by $B(M1) \approx 0.1 \mu_N^2$ which would not contradict the present results.

5. Conclusions

In conclusion, we presented a nuclear resonance fluorescence study of ^{115}In in the energy range $E_x = 2$–5 MeV. The results are compared to QPM calculations which, for the first time, include 'quasiparticle ⊗ two-phonon' configurations in the determination of the electromagnetic transition strength to excited levels in odd-mass nuclei. The extended model space leads to a considerable improvement in the description of low-lying levels. Also, the calculations are capable to account quantitatively for the (γ, γ') cross sections while results with a model space restricted to 'quasiparticle ⊗ one-phonon' states clearly overestimate it.

The successful description within the QPM leads to a somewhat different interpretation of the microscopic nature of the (γ, γ') transitions with respect to earlier results obtained with the more restricted UM approach [6], indicating a less important role of spin-flip $M1$ transitions and non-negligible $E2$ strength due to coupling of the $g_{9/2}$ g.s. configuration to the collective 2_1^+ states in the even neighbour nuclei.

What remains is a QPM application with the extended model space to interpret the structure of intermediate states observed in the photoactivation of $^{115}\mathrm{In}^m$ [6]. This necessitates the implementation of additional terms in the decay cascade calculation due to $[\alpha Q] \rightarrow [\alpha QQ]$, and vice versa, transitions. Work along these lines is in progress.

We are indebted to H.-D. Gräf and the S-DALINAC crew for their great support in the operation of the accelerator. Stimulating discussions with K. Heyde are gratefully acknowledged. One of us (V.Yu.P.) would like to thank the members of the S-DALINAC group for their hospitality during his stay at Darmstadt. This work was supported by the German Federal Minister of Research and Technology (BMFT) under contract number 06DA641I and by a grant of the Heisenberg-Landau program.

References

1. Huxel, N., Ahner, W., Diesener, H., Neumann-Cosel, P. von, Rangacharyulu, C., Richter, A., Spieler, C., Ziegler, W., De Coster, C., Heyde, K.: Nucl. Phys. A**539**, 478 (1992)
2. Bauske, I., Arias, M., Brentano, P. von, Frank, A., Friedrichs, H., Heil, R.D., Herzberg, R.-D., Hoyler, F., Van Isacker, P., Kneissl, U., Margraf, J., Pitz, H.H., Wesselborg, C., Zilges, A.: Phys. Rev. Lett. **71**, 975 (1993)
3. Zilges, A., Herzberg, R.-D., Brentano, P. von, Dönau, F., Heil, R.D., Jolos, R.V., Kneissl, U., Margraf, J., Pitz, H.H., Wesselborg, C.: Phys. Rev. Lett. **70**, 2880 (1993)
4. Collins, C.B., Carroll, J.J., Taylor, K.N., Richmond, D.G., Sinor, T.W., Huber, M., Neumann-Cosel, P. von, Richter, A., Ziegler, W.: Phys. Rev. C**46**, 952 (1992)
5. Carroll, J.J., Collins, C.B., Heyde, K., Huber, M., Neumann-Cosel, P. von, Ponomarev, V.Yu., Richmond, D.G., Richter, A., Schlegel, C., Sinor, T.W., Taylor, K.N.: Phys. Rev. C**48**, 2238 (1993)
6. Neumann-Cosel, P. von, Richter, A., Spieler, C., Ziegler, W., Carroll, J.J., Sinor, T.W., Richmond, D.G., Taylor, K.N., Collins, C.B., Heyde, K.: Phys. Lett. B**266**, 9 (1991)
7. Heyde, K., Van Isacker, P., Waroquier, M., Wood, J.L., Mayer, R.A.: Phys. Rep. **102**, 293 (1983)
8. Ponomarev, V.Yu., Dubenskiy, A.P., Dubenskiy, V.P., Boikova, E.A.: J. Phys. G**16**, 1727 (1990)
9. Dubenskiy, A.P., Dubenskiy, V.P., Boikova, E.A., Malov, L.A.: Bull. Acad. Sci. USSR Phys. Ser. **54**, 166 (1990)
10. Huber, M., Neumann-Cosel, P. von, Richter, A., Schlegel, C., Schulz, R., Carroll, J.J., Taylor, K.N., Richmond, D.G., Sinor, T.W., Collins, C.B., Ponomarev, V.Yu.: Nucl. Phys. A**559**, 253 (1993)
11. Alrutz-Ziemssen, K., Flasche, D., Gräf, H.-D., Huck, V., Knirsch, M., Lotz, W., Richter, A., Rietdorf, T., Schardt, P., Spamer, E., Stascheck, A., Voigt, W., Weise, H., Ziegler, W.: Part. Acc. **29**, 53 (1990)

12. Lindenstruth, S., Degener, A., Heil, R.D., Jung, A., Kneissl, U., Margraf, J., Pitz, H.H., Schacht, P., Seemann, U., Stock, R., Wesselborg, C.: Nucl. Instrum. Methods A**300**, 293 (1991)
13. Ziegler, W., Huxel, N., Neumann-Cosel, P. von, Rangacharyulu, C., Richter, A., Spieler, C., De Coster, C., Heyde, K.: Nucl. Phys. A**559**, 366 (1993)
14. Spieler, C.: Diploma thesis, Technische Hochschule Darmstadt 1993 (unpublished)
15. Ziegler, W.: Ph.D. thesis, Technische Hochschule Darmstadt 1990 (unpublished)
16. Brun, R., Bruyart, F., Maire, M., McPherson, A.C., Zanarini, P.: Program GEANT3.15, CERN report DD/EE/84-1 (1987)
17. Neumann-Cosel, von, Huxel, N., Richter, A., Spieler, C., Carroll, J.J., Collins, C.B.: Nucl. Instrum. Methods A**338**, 425 (1994)
18. Blachot, J., Marguir, G.: Nucl. Data Sheets **51**, 565 (1987)
19. Alston III, W.J.: Phys. Rev. **188**, 1837 (1969)
20. Boivin, M., Cauchois, Y., Heno, M., Zecevic, V.: Nucl. Phys. A**204**, 220 (1973)
21. Cauchois, Y., Ben Abdelaziz, Y., Khérouf, R., Schloesing-Möller, J.: J. Phys. G**7**, 1539 (1981)
22. Vdovin, A.I., Voronov, V.V., Soloviev, V.G., Stoyanov, Ch.: Sov. J. Part. Nucl. **16**, 105 (1985); Galès, S., Stoyanov, Ch., Vdovin, A.I.: Phys. Rep. **166**, 125 (1988)
23. Khuong, C.Z., Soloviev, V.G., Voronov, V.V.: J. Phys. G**7**, 151 (1981)
24. Malov, L.A., Soloviev, V.G.: Sov. J. Nucl. Phys. **21**, 263 (1975)
25. Heyde, K., Waroquier, M., Meyer, R.A.: Phys. Rev. C**17**, 1219 (1978)
26. Bernard, V., Giai, Nguyen V.: Nucl. Phys. A**348**, 75 (1980); Bortignon, P.F., Broglia, R.A.: Nucl. Phys. A**371**, 405 (1981)
27. Klevansky, S.A., Lemmer, R.H.: Phys. Rev. C**28**, 1763 (1983); Matveev, B.B., Tulupov, B.A., Muraviev, S.E., Urin, M.G.: Phys. Lett. B**167**, 255 (1986)
28. Soloviev, V.G., Malov, L.A.: Nucl. Phys. A**196**, 433 (1972)
29. Stoyanov, Ch., Khuong, C.Z.: JINR Dubna Report P4-81-234 (1981) (unpublished)
30. Milkau, U., Bohle, D., Richter, A.: Nucl. Phys. A**499**, 517 (1989)